Surface Catalyzed Oxidative Oligomerization of 17β–Estradiol by Fe 3+ –Saturated Montmorillonite

6 AUTHORS, INCLUDING:

Chao Qin

Virginia Polytechnic Institute and State Univer…

4 PUBLICATIONS **45** CITATIONS

SEE PROFILE

Chao Shang

Virginia Polytechnic Institute and State Univer…

56 PUBLICATIONS **737** CITATIONS

SEE PROFILE

Richard F Helm

Virginia Polytechnic Institute and State Univer…

114 PUBLICATIONS **2,627** CITATIONS

SEE PROFILE

Surface Catalyzed Oxidative Oligomerization of 17β-Estradiol by Fe³⁺-Saturated Montmorillonite

Chao Qin,[†] Diego Troya,[‡] Chao Shang,[†] Sherry Hildreth,[§] Rich Helm,[§] and Kang Xia*[,†]

[†]Department of Crop and Soil Environmental Sciences, [‡]Department of Chemistry, [§]Department of Biochemistry, Virginia Polytechnic Institute and State University, Blacksburg, Virginia 24061, United States

Ⓢ *Supporting Information*

ABSTRACT: With widespread detection of endocrine disrupting compounds including hormones in wastewater, there is a need to develop cost-effective remediation technologies for their removal from wastewater. Previous research has shown that Fe³⁺-saturated montmorillonite is effective in quickly transforming phenolic organic compounds such as pentachlorophenol, phenolic acids, and triclosan via surface-catalyzed oligomerization. However, little is known about its effectiveness and reaction mechanisms when reacting with hormones. In this study, the reaction kinetics of Fe³⁺-saturated montmorillonite catalyzed 17β-estradiol (βE2) transformation was investigated. The transformation products were identified using liquid chromatography coupled with mass spectrometry, and their structures were further confirmed using computational approach. Rapid βE2 transformation in the presence of Fe³⁺-saturated montmorillonite in an aqueous system was detected. The disappearance of βE2 follows first-order kinetics, while the overall catalytic reaction follows the second-order kinetics with an estimated reaction rate constant of 200 ± 24 (mmol βE2/g mineral)$^{-1}$ h^{-1}. The half-life of βE2 in this system was estimated to be 0.50 ± 0.06 h. βE2 oligomers were found to be the major products of βE2 transformation when exposed to Fe³⁺-saturated montmorillonite. About 98% of βE2 were transformed into βE2 oligomers which are >10^7 times less water-soluble than βE2 and, therefore, are much less bioavailable and mobile then βE2. The formed oligomers quickly settled from the aqueous phase and were not accumulated on the reaction sites of the interlayer surfaces of Fe³⁺-saturated montmorillonite, the major reason for the observed >84% βE2 removal efficiency even after five consecutive usages of the same of Fe³⁺-saturated montmorillonite. The results from this study clearly demonstrated that Fe³⁺-saturated montmorillonite has a great potential to be used as a cost-effective material for efficient removal of phenolic organic compounds from wastewater.
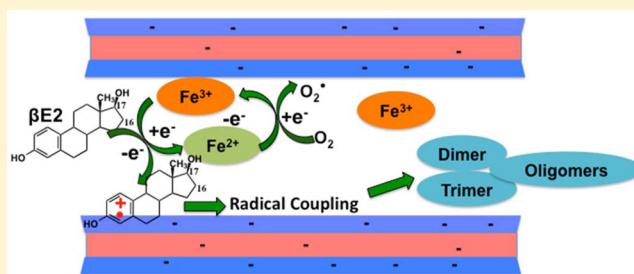
INTRODUCTION

The prevalent worldwide detection of endocrine disrupting compounds (EDCs) in the aquatic environment[1−4] as well as in drinking water[5,6] have caused increasing concerns about their adverse environmental impact. Natural estrogens including 17β-estradiol (βE2) are of particular environmental concern among EDCs because they can negatively affect certain aquatic organisms at a level as low as 10 ng/L, which is orders of magnitude lower than the lowest observed adverse effect levels (LOAEL) for other anthropogenic EDCs.[7] The adverse impact of estrogens on aquatic organisms includes fish egg production inhibition and sex reversal of males, which ultimately could result in the collapse of local fish populations.[8−10]

Municipal wastewater treatment plants (WWTP) are one of the major sources contributing to elevated natural estrogens in the environment.[11,12] Research has demonstrated that existing wastewater treatment technologies are not effective at removing estrogens to levels below biological significance.[13,14] Significant effort has been made to develop wastewater treatment technologies capable of reducing levels of estrogens and other EDCs in treated wastewater to environmental insignificant levels before wastewater effluent is released into the environ-

ment.[15−17] While treatment technologies utilizing granular activated carbon (GAC), ozonation, and chlorine dioxide have provided promising results for effective removal of estrogens from WWTP effluents,[18] the application of those treatment technologies has been restricted by high cost of installation and maintenance.[13]

Recent research has shown that Fe³⁺-saturated montmorillonite can rapidly transform phenolic organic compounds such as pentachlorophenol, phenolic acids, and triclosan via surface-catalyzed oligomerization.[19−21] Compared to parent compounds, the oligomerized compounds are much less water-soluble and, therefore, less bioavailable or biologically active.[22] Montmorillonite, a 2:1 layered aluminosilicate mineral that is widely distributed worldwide,[23] has enormous potential as a platform for nanoscale surface catalyzed chemical reactions.[24,25] In aqueous environment, the interlayer cations of montmorillonite attract water, resulting in an expansion of the interlayer

spacing to approximately 4−10 Å depending on the type of interlayer cations.[26−28] This interlayer space is wide enough for small size organic molecules such as βE2 (12 Å × 6 Å × 4 Å, Table S1, Supporting Information) to move into the interlayer space, and it also provides a large interlayer surface area that allows surface-catalyzed reactions for organic molecules. The mechanisms of montmorillonite surface catalyzed chemical reactions involve reduction of mineral interlayer cations such as Cu^{2+} and Fe^{3+} and oxidation of organic compounds resulting in organic compound radicals that are highly susceptible to further oligomerization and/or degradation reactions.[29,30] The objective of this study was to investigate, using experimental and computational approaches, the transformation kinetics and pathways of βE2 transformation catalyzed by Fe^{3+}-saturated montmorillonite. Because it has the highest estrogenic activity among estrogens, βE2 was selected as the representative compound for this investigation.

MATERIALS AND METHODS

Chemicals and Materials. Estrone (E1) (≥99%) and 17β-estradiol (βE2) (≥98%) were purchased from Sigma-Aldrich (St. Louis, MO). Ferric chloride (hexahydrate, ≥97%), HPLC grade acetonitrile, ethyl acetate, and acetone were purchased from Fisher Scientific (Fair Lawn, NJ). Na-montmorillonite (SWy-2, Crook County, Wyoming) was obtained from the Source Clays Repository of the Clay Minerals Society (Purdue University, West Lafayette, IN). The cation exchange capacity and theoretical external surface area of SWy-2 provided by the Clay Minerals Society were 76.4 cmol$_c$/kg and 31.82 ± 0.22 m^2/g, respectively. The ultrapure water used in this study was produced by Millipore Milli-Q water purification system (Milford, MA).

Fe^{3+}-Saturated Montmorillonite Preparation. Na-montmorillonite (SWy-2) was fractionated to <2 μm clay-sized particles before Fe^{3+} saturation following the procedure in Arroyo et al.[31] 10 g of <2 μm Na-montmorillonite was then mixed with 400 mL of 0.1 M FeCl$_3$ on a magnetic stir plate for 8 h before centrifugation at 4500 rpm for 20 min. The sediment was resuspended in another 400 mL of 0.1 M FeCl$_3$. The above procedure was repeated six times in order to saturate the montmorillonite interlayer with Fe^{3+}. The Fe^{3+}-saturated montmorillonite was then repeatedly washed with 100 mL HPLC grade water followed by centrifugation at 4500 rpm for 20 min until no Cl$^-$ was detected in the supernatant with an AgNO$_3$ test. Removal of Cl$^-$ from the system indicates the removal of other cations such as Na$^+$ and Ca^{2+}, which can compete with Fe^{3+} for the interlayer surface sites. The washed Fe^{3+}-saturated montmorillonite was finally freeze-dried for future experiment use. More details for preparation of Fe^{3+}-saturated montmorillonite can be found elsewhere.[21]

Reaction of βE2 with Fe^{3+}-Saturated Montmorillonite. One hundred μL of βE2 stock solution (βE2 dissolved in acetone at 1.36 mg/mL) was mixed with 50 mg of Fe^{3+}-saturated montmorillonite in 20 mL glass vials to produce an initial concentration of 0.01 mmol of βE2/g of mineral. After complete evaporation of acetone, a carrier solvent, from glass vials under a fume hood, 1.5 mL of ultrapure water was added into each glass vial and shaken in darkness at 25 °C on an incubator shaker at 120 rpm for up to 10 days. The pH of Milli-Q water was 6.3, which is close to the typical domestic wastewater before treatment (pH ranges from 6.5 to 8.5). A similar experimental procedure was conducted using Na-montmorillonite. The same amount of βE2 was added to a 1.5 mL FeCl$_3$ solution which contained the same amount of Fe^{3+} as that in the Fe^{3+}-saturated montmorillonite system (determined as 0.997 mmol Fe^{3+}/g montmorillonite). There were triplicates per treatment. At given intervals, triplicate vials from each treatment were collected, and the content of each vial was immediately analyzed for βE2 and its transformation products using the methods described below.

Extraction Method. Upon termination of the reaction, each collected sample was centrifuged at 4000 rpm for 30 min. The supernatant of each centrifuged sample was collected and filtered through a 0.2 μm Thermo PVDF filter before HPLC analysis for βE2 and E1. The remaining sediment of each sample was then freeze-dried for 15 min, mixed with 3 mL of ethyl acetate, sonicated for 30 min, and then centrifuged at 4000 rpm for 30 min. One mL of ethyl acetate extract of each sample was collected and then evaporated to dryness using a Vacuum Evaporator (RapidVap, Labconco) at 35 °C. The dried residue was redissolved in 1 mL of acetonitrile and water (v/v, 40:60) and filtered through a 0.2 μm Thermo PTFE filter before HPLC analysis for βE2 and LC/MS/MS analysis for E1. The amount of βE2 transformed at the termination of the experiment was calculated by

βE2 added − (βE2 remained in the aqueous phase + βE2 remained in the sediment phase)

HPLC Analysis of βE2. The βE2 in the aqueous phase and sediment extracts was quantified using a HPLC system coupled with a fluorescence detector (Agilent 1260 Infinity, Agilent Co., CA, USA). The analytical column was EC-C18 column (3.0 × 50 mm, 2.7 μm, Agilent Poroshell 120). The mobile phase consisted of acetonitrile/water (v/v, 60:40). The mobile phase flow rate was 0.5 mL/min. The column temperature was maintained at 30 °C, and the injection volume was 20 μL. βE2 was detected by the fluorescence detector at an excitation wavelength of 280 nm and an emission wavelength of 310 nm. The limit of detection (LOD) and the limit of quantification (LOQ) were determined as 10 and 25 ppb, respectively.

Identification of βE2 Transformation Products. Transformation products were not detected in the aqueous phase at the termination of experiment. The βE2 transformation products in the ethyl acetate extracts of the sediment phase were identified using a liquid chromatography-triple quadrupole mass spectrometer (6490 LC/QQQ, Agilent Co., CA, USA). Electron spray negative ionization mode was used. Total ionization chromatography was collected in the m/z range of 50−1400. The analytical column was Eclipse C18 column (3.0 × 50 mm, Agilent). The mobile phase gradient was programmed as 0−6 min, 30% acetonitrile and 70% water; 6−22 min, 60% acetonitrile and 40% water; 22−22.5 min, 80% acetonitrile and 20% water; 22.5−24.5 min, 90% acetonitrile and 10% water; 24.5−25 min, 30% acetonitrile and 70% water. The mobile phase flow rate was 0.4 mL/min. The injection volume was 10 μL. The column temperature was maintained at 40 °C. The MS parameters were as follows: probe capillary voltage at 3.5 kV, sheath gas flow at 8 L/min, nebulizer pressure at 45 psi. The accurate masses of transformation products were further confirmed using ultra performance liquid chromatography-quadrupole-time-of-flight mass spectrometry (UPLC-Q-TOF, Waters Acquity I-class UPLC coupled with a Synapt G2-S High Definition Mass Spectrometer, Waters Corp., Milford, MA) in electron negative ionization mode. Further details on the instrumental parameters can be found in the Supporting Information.

Computational Study. All geometry optimizations for the βE2 monomer and all possible dimer and trimer species resulting from the catalyzed coupling reactions in Fe^{3+}-saturated montmorillonite were carried out with the B3LYP density functional theory (DFT) method and the 6-31G* basis set as implemented in the Gaussian09 suite of programs. The relative energies of all dimer and trimer isomers were used to evaluate the thermodynamic stability of all the possible βE2 transformation products.

■ RESULTS AND DISCUSSION

Kinetics of Fe^{3+}-Saturated Montmorillonite Catalyzed βE2 Transformation. As shown in Figure 1, in the presence of
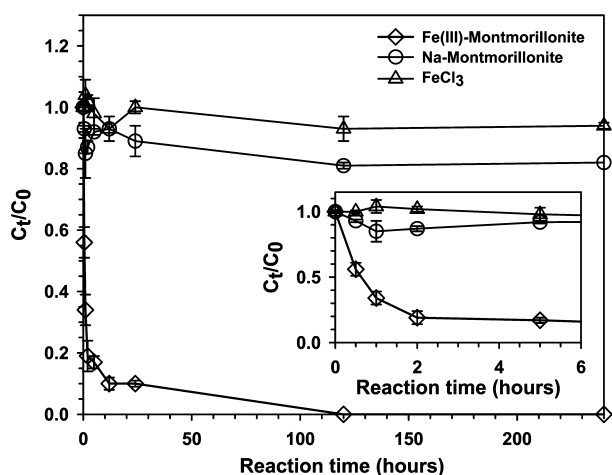
Figure 1. βE2 transformation kinetics in aqueous systems containing Fe^{3+}-saturated montmorillonite, Na^+-montmorillonite, and 33.2 mM $FeCl_3$. The initial βE2 concentration was 0.01 mmol βE2/g of mineral. The amount of Fe^{3+} in the $FeCl_3$ system was equivalent to the amount of Fe^{3+} saturated on the montmorillonite.

Fe^{3+}-saturated montmorillonite, βE2 rapidly disappeared within the first 2 h following first-order kinetics with an estimated overall second-order reaction rate constant of 200 ± 24 (mmol βE2/g mineral)$^{-1}$ h^{-1}. The half-life of βE2 in this system was estimated to be 0.50 ± 0.06 h. Within the first 2 h only 20% of initially added βE2 remained. Close to 100% of the initially added βE2 was transformed on the fifth day. However, transformation of βE2 was much slower in the presence of Na-montmorillonite compared to the system containing Fe^{3+}-saturated montmorillonite. Even after 10 days, about 82% of initially added βE2 still remained in the Na-montmorillonite system. When βE2 was incubated with $FeCl_3$ solution that contained the same amount of Fe^{3+} that was saturated in the montmorillonite system, close to 94% of initially added βE2 remained in the system after 10 days, indicating limited βE2 transformation.

Previous studies had investigated reaction of aromatic compounds with transition metal cations (e.g., Fe^{3+}, Cu^{2+}) saturated montmorillonite.[19,20,32−35] The results lead to the proposal that during the reaction, electrons were donated by the unsaturated organic compounds to the metal cations sorbed on the negatively charged interlayer surfaces of montmorillonite, resulting in formation of radical cations of aromatic molecules and reduced metal cations such as Fe^{2+}, Cu^+, which can be oxidized back to Fe^{3+}, Cu^{2+} in aerobic conditions.[32,34,36]

The formed organic radicals are not stable and can be further degraded[32] or oligomerized.[33,37]

The observed rapid βE2 transformation in the Fe^{3+}-saturated montmorillonite system (Figure 1) suggests redox reactions between βE2 and Fe^{3+}, similar to the mechanism proposed by previous studies.[20,21] Because the lone pair electrons on the phenolic functional group and the benzene ring π cloud of βE2 structure are conjugated, the phenolic functional group is prone to undergo an electron-transfer reaction with Fe^{3+} to form a free βE2 radical. The unpaired electron of the resulting βE2 radical may delocalize through resonance to the respective conjugated positions of the neighboring benzene ring. The data shown in Figure 1 further demonstrated that the redox reaction is mainly facilitated and enhanced by mineral surface chemistry based on the fact that less than 6% of βE2 was removed in the Na-montmorillonite aqueous system as well as in the $FeCl_3$ solution, where Fe^{3+} was not sorbed to montmorillonite surfaces in both systems.

Although Na-montmorillonite naturally contains structural Fe(III) evenly distributed in the octahedral layers of the mineral at a concentration of approximately 0.61 mmol Fe(III)/g mineral,[38] the inaccessibility of the Fe(III) trapped in the octahedral layer and lack of surface reaction sites with Fe^{3+} contributed to the limited and slow βE2 transformation in the Na-montmorillonite system (Figure 1). Microbial contribution to the βE2 transformation in the Na-montmorillonite system, although expected to be low, cannot be excluded without additional microbial activity characterization. In the $FeCl_3$ solution, the phenolic group of βE2 interact with Fe^{3+} via outer sphere complexation,[19] resulting in limited electron transfer from βE2 to Fe^{3+} because of the aqueous layer around Fe^{3+}. In the Fe^{3+}-saturated montmorillonite system, the planar negatively charged montmorillonite interlayer surfaces catalyze the oxidative transformation of βE2 by surface sorbed Fe^{3+}, most likely via enhancement of precursor inner sphere complexation of the organic reductant and the metal oxidant and the associated electron transfer within a precursor complex,[39] resulting in the formation of βE2 radicals and their further transformation.

βE2 Transformation Products-Experimental Observation. The products formed during Fe^{3+}-saturated montmorillonite mediated βE2 transformation were characterized using LC/MS. The LC/triple quadruple MS extracted ion chromatograms of a sample collected 5 days after βE2 was incubated with Fe^{3+}-saturated montmorillonite are shown in Figure 2. In addition to parent compound βE2 ([M−H]$^-$, m/z = 271), peaks with m/z = 269, 541, 811, and 1081 were observed (Figure 2). The appearance of peak with m/z = 269 indicates the formation of deprotonated E1 ([M−H]$^-$) during βE2 transformation. The five peaks (D_1-D_5) with a retention time of 4.12, 4.87, 5.36, 5.60, and 7.06 min each has m/z = 541, suggesting formation of βE2 dimers with molecular weight of 542 (βE2 × 2-2H = 542). The three peaks (T_1-T_3) clustered between 6.50 and 7.50 min in Figure 2 each has m/z = 811, indicating formation of βE2 trimers with molecular weight of 812 (βE2 × 3-4H = 812). The broad peak appearing at retention time of 11.50 min has m/z = 1081, suggesting a molecular mass of 1082, which corresponds to the βE2 tetramer (272 × 4-6H = 1082). Table 1 shows a close match between the theoretical molecular mass of the proposed βE2 transformation products and those detected using a UPLC-ESI-Q-TOF.
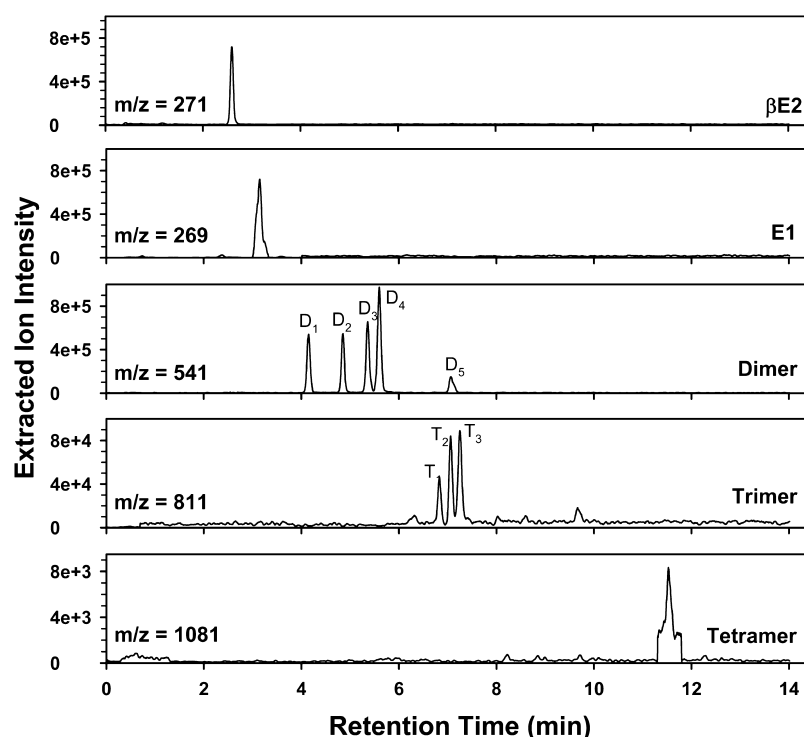
Figure 2. LC/MS extracted ion chromatograms of compounds in a sample collected 5 days after βE2 was incubated with Fe^{3+}-saturated montmorillonite.

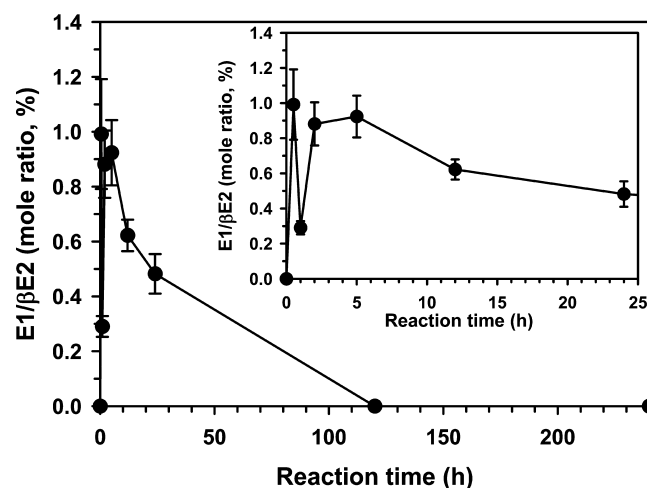**Table 1. Accurate Mass Measurement of βE2 Transformation Products in the Fe^{3+}-Saturated Montmorillonite System**

products[a]		retention time (min)	formula	molecular mass (u)	
				experimental[b]	theoretical
βE2		2.597	$C_{18}H_{24}O_2$	272.21	272.38
E1		3.238	$C_{18}H_{22}O_2$	270.21	270.16
βE2 dimers	D_1	4.119	$C_{36}H_{46}O_4$	542.3386	542.3396
	D_2	4.873			
	D_3	5.358			
	D_4	5.604			
	D_5	7.059			
βE2 trimers	T_1	6.828	$C_{54}H_{68}O_6$	812.5013	812.5016
	T_2	7.067			
	T_3	7.261			
tetramer		11.544	$C_{72}H_{90}O_8$	1082.6660	1082.6636

[a]Peaks are shown in Figure 2. [b]Mass spectra are shown in Figures S1, S2, and S3.

Figure 3. Formation kinetics of E1 during βE2 reaction with Fe^{3+}-saturated montmorillonite. The initial βE2 concentration was 0.01 mmol βE2/g of mineral.

As shown in Figure 3, in the Fe^{3+}-saturated montmorillonite system the production of E1 rapidly increased initially, reached to peak level after 0.5 h, and then disappeared from the system at day 5. Compared to the amount of βE2 initially added to the system, only a small fraction of E1 was produced, with a maximum mole ratio of E1/E2 at 0.99 ± 0.20% after 0.5 h of reaction when the E1 level reached its maximum. Previous research has shown that E1 produced by oxidation of βE2 can be quickly converted back to βE2 via reduction.[40,41] It is possible that oxidation of the Fe^{2+} produced from the Fe^{3+}-E2 redox reaction quickly reduced E1 back to βE2.

Due to lack of analytical standards, βE2 dimer, trimer, and tetramer levels were not quantified. As shown in Figure 4, the sum of five dimer peak areas, an indicator of detected level of all

five dimers in the ethyl acetate extract of sediment phase, increased rapidly and reached the maximum within the first hour of reaction. The total peak area of all five dimers decreased after 2 h and remained unchanged up to 5 h. Its level went back up slightly at 12 h followed by a steady decrease thereafter but remained detectable at 10 days. A similar trend was observed for the peak area sum of the three trimers for the first 12 h of reaction; however, its level remained constant between 12 h and 5 days of reaction. After 10 days of reaction, the peak sum of trimers decreased slightly but also remained detectable (Figure 4). The peak area ratio of ethyl acetate extractable dimers and trimers decreased sharply from around 65 at 0.5 h to 24 at 1 h and slowly decreased thereafter to
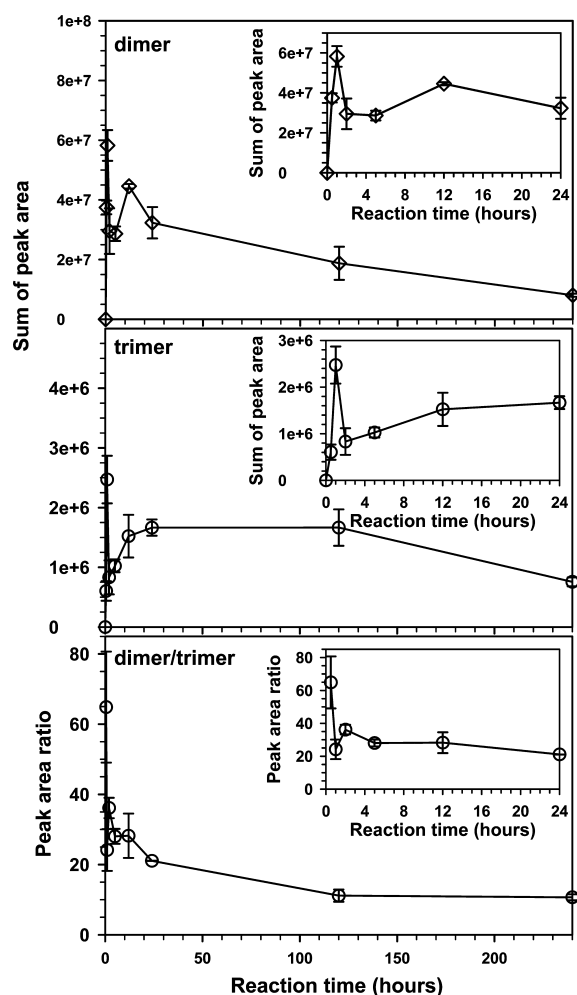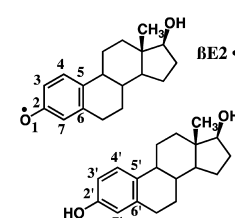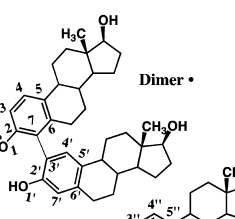
Figure 4. Formation kinetics of dimers and trimers during βE2 reaction with Fe^{3+}-saturated montmorillonite. The initial βE2 concentration was 0.01 mmol βE2/g of mineral.

Table 2. Relative Molecular Energy for βE2 Dimers and Trimers[a]

	Example of molecular structure of parent compounds	Bonding positions	Relative energy* (kcal/mol)
Dimers		7-3'	0.0
		3-7'	0.2
		3-3'	0.6
		1-3'	2.1
		7-7'	3.9
		1-7'	5.5
		3-1'	5.9
		7-1'	6.0
Trimers		7-3', 3-3''	0.0
		3-3', 7-7''	1.0
		7-3', 3-7''	3.1
		7-7', 3-3''	3.2
		3-3', 7-3''	3.6

[a]The asterisk denotes the following: relative energy referred to the lowest energy of a compound within the same oligomer series.

around 11 after 5 days of reaction and remained unchanged until day 10 (Figure 4). This observation suggests that after βE2 dimers were formed initially some of them were further transformed to trimers, while some of the trimers were further transformed into other products, resulting in relatively steady dimer/trimer peak area ratio at longer reaction time. The observation of tetramer production (Figure 2, Table 1) confirms that some trimers were further transformed into tetramers. It is suspected that the low detectable level of ethyl acetate extractable tetramers, as reflected in the small peak area of the broad tetramer peak shown in Figure 2, was mostly due to decreased solvent solubility/extractability with increased chain length of oligomers.

As shown in Table S3 of the Supporting Information, the calculated water solubility of βE2 dimers, trimers, and tetramers are about 1.6×10^2, 1.7×10^5, and 2.3×10^7 times, respectively, lower than that for βE2 (23.7 mg/L). It is most likely that the oligomers were settled with the mineral phase once formed during the reaction and were too insoluble to be extracted by any solvents, resulting in their no-detection on LC/MS. To test this hypothesis, the organic C content in the sediment after 5 days of reaction between βE2 and Fe^{3+}-saturated montmorillonite was determined. The amount of organic C detected in the 5-day sediment samples was on average about 98.1% of that in the βE2 initially added to the system. As shown in Figure 1,

about 99.7% of initially added βE2 was transformed at day 5, suggesting most of the βE2 transformation products were settled with the mineral phase, most likely as highly insoluble βE2 oligomers. The X-ray diffraction (XRD) data in Table S2 of the Supporting Information shows that the difference between the interlayer spacing of freeze-dried sediment collected from βE2 + Fe^{3+}-saturated montmorillonite system after 5-day reaction was only 0.3 Å larger than that of freeze-dried sediment from the Fe^{3+}-saturated montmorillonite only system. Considering that the average dimensions of dimers and trimers are 17 Å × 10 Å × 7 and 20 Å × 15 Å × 9 Å, respectively (Table S3, Supporting Information) and even larger dimensions for higher oligomers, it is unlikely that the formed oligomers are trapped in between the interlayer spacing of Fe^{3+}-saturated montmorillonite. Instead, the XRD data suggests the possibility that the βE2 oligomers formed at the interlayer spacing of Fe^{3+}-saturated montmorillonite could be easily separated from the mineral surfaces during extraction and settled on their own with the mineral sediment.

βE2 Transformation Products-Computational Characterization. The LC/MS results demonstrated that the molecular mass of detected βE2 oligomer products followed the pattern of $nM - 2(n - 1)$ (Table 1), where n is the number of coupling βE2 monomer and M is the molecular mass of βE2. Such pattern often indicates radical coupling reactions, where a dimer is formed by covalent bonding of two parent monomers with elimination of two hydrogen atoms.[22] The dimers could further undergo coupling reactions and yield larger oligomers.[22,42,43] To further identify possible structures of βE2 dimers and trimers, relative thermodynamic stability of
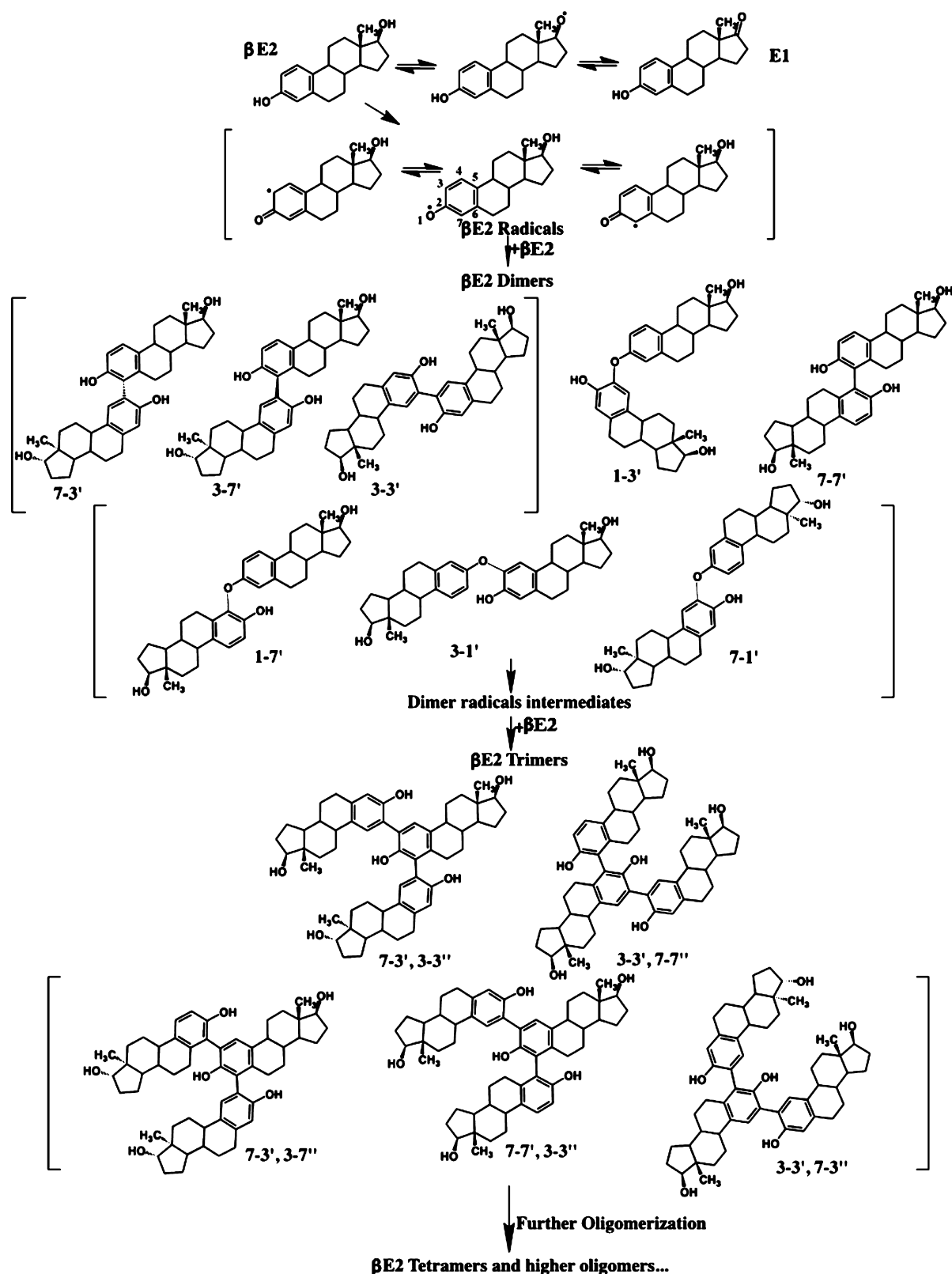
Figure 5. Proposed reaction pathways for Fe^{3+}-saturated montmorillonite catalyzed βE2 oligomerization.

βE2 dimer and trimer products were computed using electronic structure calculations (Table 2). Because the number of possible isomers for the association of four or more βE2 radicals grows intractably large, computational exploration of oligomers other than dimers and trimers was not approached.

Based on the spin and charge density computational results published by Mao et al.,[44] possible coupling products were predicted and the relative energy of each coupling products was calculated. The computational results suggested that βE2 dimers were most likely formed by the bond coupling of
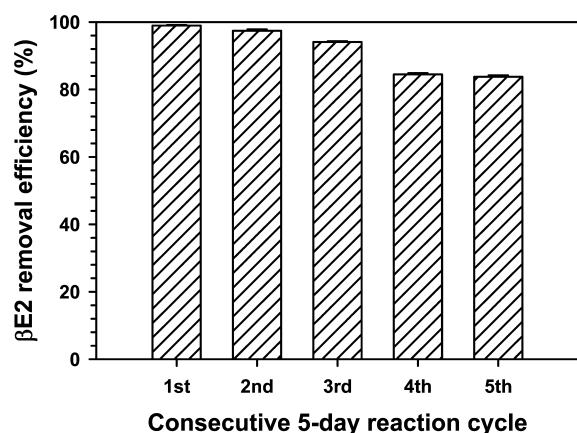
Figure 6. βE2 removal efficiency of consecutive 5-day reaction cycles using the same Fe^{3+}-saturated montmorillonite. The concentration of βE2 at the beginning of each reaction cycle was 0.01 mmol βE2/g of mineral.

unsubstituted O1, C3, and C7 on the phenolic ring of a βE2 radical with those on the second βE2 to form eight dimer conformers as listed in Table 2. The computer-optimized relative energy for the eight dimer conformers listed in Table 2 shows that 7-3′, 3-7′, and 3-3′ dimer coupling species have similar relative energies and the highest thermodynamic stability, indicating their highest possibility of formation compared to other species during the reaction. Compared to the relative energies of the three most likely formed dimer species, the relative energy of 1-3′, 7-7′, and 1-7′ dimer coupling species increased by 1.5, 3.3, and 4.9 kcal/mol, respectively. The relative energies for the 3-1′ and 7-1′ dimer coupling species are similar, and both are slightly higher than that for the 1-7′ dimer. The ranking of the calculated relative energy of the dimer species (Table 2) suggests the formation possibility of dimer coupling species as 7-3′ ≈ 3-7′ ≈ 3-3′ > 1-3′ > 7-7′ > 1-7′ > 3-1′ ≈ 7-1′. Dimer conformers with 7-3′, 3-7′, 3-3′, 1-3′, and 7-7′ bond couplings were also observed by NMR for oxidative coupling reactions of βE2 in laccase or peroxidase/H_2O_2 systems.[45,46]

Computational results showed that a βE2 trimer was slightly more likely formed by the coupling reaction of a βE2 dimer radical to a neutral βE2 molecule rather than the coupling reaction between a βE2 radical and a neutral βE2 dimer because the relative energy of the former reaction is on average 1.8 kcal/mol lower than that of the later reaction scenario. Table 2 lists five trimer conformers with the lowest relative energies among all possible trimer products. The formation possibility of trimer coupling species are (7-3′, 3-3″) > (3-3′, 7-7″) > (7-3′, 3-7″) ≈ (7-7′, 3-3″) ≈ (3-3′, 7-3″). Figures S4 and S5 of the Supporting Information illustrate the optimized molecular structures of dimers and trimers listed in Table 2.

The experimental data of this paper suggest that βE2 oligomers are the major products of reaction between βE2 and Fe^{3+}-saturated montmorillonite in an aqueous system. The βE2 oligomerization is catalyzed by the Fe^{3+} sorbed on montmorillonite interlayer surfaces, producing highly insoluble βE2 oligomers. Using the relative thermodynamic stability predicted by electronic structure calculations, a schematic of the plausible reaction pathways is shown in Figure 5.

Environmental Implication. This study provided, for the first time, experimental evidence that ~98% of βE2 was transformed into highly water insoluble oligomers in an

aqueous system containing Fe^{3+}-saturated montmorillonite and at a pH level that is similar to the pH range (6.5 to 8.5) of typical domestic wastewater. With an estimated reaction rate constant of ~200 (mmol E2/g mineral)$^{-1}$ h^{-1} and a half-life of ~0.50 h, Fe^{3+}-saturated montmorillonite can potentially be used for removal of βE2 and other hormones during wastewater treatment processes. The βE2 oligomers, which are >10^7 times less water-soluble than βE2 (Table S3, Supporting Information), can be settled out of the aqueous phase during wastewater treatment processes and become much less bioavailable and mobile than the parent compound. Previous research has shown that triclosan dimers and trimers formed in the presence of Fe^{3+}-saturated montmorillonite exhibited high chemical stability in highly oxidative and reductive conditions,[47] implying that other oligomers formed in similar reactions could potentially be stable under natural environment conditions.

In addition, because oligomers are not accumulated over the reaction sites on the interlayer surfaces of Fe^{3+}-saturated montmorillonite, it is possible for the oligomerization reaction at the reaction sites to occur repeatedly, resulting in extended effectiveness of Fe^{3+}-saturated montmorillonite for removal of contaminants from wastewater. As shown in Figure 6, even after five consecutive 5-day reaction cycles using the same Fe^{3+}-saturated montmorillonite and the same initial level of βE2 at each cycle, the βE2 removal efficiency remained at >84%.

It is important to point out that βE2 concentration much higher than that detected in typical WWTP effluents was used for this study because the focus of this study was to assess the capacity of the Fe^{3+}-saturated montmorillonite to polymerize βE2 and to understand the reaction pathways. Investigation on the concentration dependence of this reaction is important and would warrant a separate study. Our previous investigation on Fe^{3+}-saturated montmorillonite catalyzed polymerization of triclosan (TCS) demonstrated inverse correlation between TCS half-life and initial TCS concentration.[21] Reduction of 30 times in initial TCS concentration resulted in 400% reduction in TCS half-life. Similar inverse correlation between reaction rate and initial concentration is, therefore, expected for Fe^{3+}-saturated montmorillonite catalyzed polymerization of βE2. The half-life of E2 in the current study using high initial E2 concentration was about 0.5 h. Its half-life is expected to be much shorter than 0.5 h at lower initial E2 concentrations based on the result from our previous investigation.[21] However, even 0.5 h is well within the 1−5 day hydraulic retention time in typical secondary wastewater treatment plants.[48]

In summary, because montmorillonite is a widely distributed mineral worldwide, the preparation of Fe^{3+}-saturated montmorillonite is straightforward and low cost, and Fe^{3+}-saturated montmorillonite has a fast removal rate, high removal efficiency, and repeated usage; it has a great potential as a cost-effective material for effective removal of phenolic organic compounds from domestic wastewater as well as animal lagoon effluent.

■ ASSOCIATED CONTENT

Ⓢ Supporting Information
Text, Figures S1−S5, and Tables S1−S4. This material is available free of charge via the Internet at http://pubs.acs.org.

AUTHOR INFORMATION

Corresponding Author

*Phone: 1540 231 9323. E-mail: kxia@vt.edu. Corresponding author address: Department of Crop and Soil Environmental Sciences, Virginia Tech, 1880 Pratt Dr., Blacksburg, VA 24061.

Notes

The authors declare no competing financial interest.

REFERENCES

(1) Kolpin, D. W.; Furlong, E. T.; Meyer, M. T.; Thurman, E. M.; Zaugg, S. D.; Barber, L. B.; Buxton, H. T. Pharmaceuticals, hormones, and other organic wastewater contaminants in US streams, 1999−2000: A national reconnaissance. *Environ. Sci. Technol.* **2002**, *36* (6), 1202−1211.

(2) Yamamoto, A.; Kakutani, N.; Yamamoto, K.; Kamiura, T.; Miyakoda, H. Steroid hormone profiles of urban and tidal rivers using LC/MS/MS equipped with electrospray ionization and atmospheric pressure photoionization sources. *Environ. Sci. Technol.* **2006**, *40* (13), 4132−4137.

(3) Chang, H.; Wan, Y.; Hu, J. Determination and source apportionment of five classes of steroid hormones in urban rivers. *Environ. Sci. Technol.* **2009**, *43* (20), 7691−7698.

(4) Stasinakis, A. S.; Gatidou, G.; Mamais, D.; Thomaidis, N. S.; Lekkas, T. D. Occurrence and fate of endocrine disrupters in Greek sewage treatment plants. *Water Res.* **2008**, *42* (6), 1796−1804.

(5) Benotti, M. J.; Trenholm, R. A.; Vanderford, B. J.; Holady, J. C.; Stanford, B. D.; Snyder, S. A. Pharmaceuticals and endocrine disrupting compounds in US drinking water. *Environ. Sci. Technol.* **2008**, *43* (3), 597−603.

(6) Fan, Z.; Hu, J.; An, W.; Yang, M. Detection and Occurrence of Chlorinated Byproducts of Bisphenol A, Nonylphenol, and Estrogens in Drinking Water of China: Comparison to the Parent Compounds. *Environ. Sci. Technol.* **2013**, *47* (19), 10841−10850.

(7) Routledge, E. J.; Sheahan, D.; Desbrow, C.; Brighty, G. C.; Waldock, M.; Sumpter, J. P. Identification of estrogenic chemicals in STW effluent. 2. In vivo responses in trout and roach. *Environ. Sci. Technol.* **1998**, *32* (11), 1559−1565.

(8) Thorpe, K. L.; Maack, G.; Benstead, R.; Tyler, C. R. Estrogenic wastewater treatment works effluents reduce egg production in fish. *Environ. Sci. Technol.* **2009**, *43* (8), 2976−2982.

(9) Lange, A.; Paull, G. C.; Hamilton, P. B.; Iguchi, T.; Tyler, C. R. Implications of persistent exposure to treated wastewater effluent for breeding in wild roach (Rutilus rutilus) populations. *Environ. Sci. Technol.* **2011**, *45* (4), 1673−1679.

(10) Kidd, K. A.; Blanchfield, P. J.; Mills, K. H.; Palace, V. P.; Evans, R. E.; Lazorchak, J. M.; Flick, R. W. Collapse of a fish population after exposure to a synthetic estrogen. *Proc. Natl. Acad. Sci. U. S. A.* **2007**, *104* (21), 8897−8901.

(11) Griffith, D. R.; Kido Soule, M. C.; Matsufuji, H.; Eglinton, T. I.; Kujawinski, E. B.; Gschwend, P. M. Measuring Free, Conjugated, and Halogenated Estrogens in Secondary Treated Wastewater Effluent. *Environ. Sci. Technol.* **2014**, *48* (5), 2569−2578.

(12) Combalbert, S.; Hernandez-Raquet, G. Occurrence, fate, and biodegradation of estrogens in sewage and manure. *Appl. Microbiol. Biotechnol.* **2010**, *86* (6), 1671−1692.

(13) Baynes, A.; Green, C.; Nicol, E.; Beresford, N.; Kanda, R.; Henshaw, A.; Churchley, J.; Jobling, S. Additional Treatment of Wastewater Reduces Endocrine Disruption in Wild Fish · A Comparative Study of Tertiary and Advanced Treatments. *Environ. Sci. Technol.* **2012**, *46* (10), 5565−5573.

(14) Ings, J. S.; Servos, M. R.; Vijayan, M. M. Hepatic transcriptomics and protein expression in rainbow trout exposed to municipal wastewater effluent. *Environ. Sci. Technol.* **2011**, *45* (6), 2368−2376.

(15) Eggen, R. I. L.; Hollender, J.; Joss, A.; Schärer, M.; Stamm, C. Reducing the Discharge of Micropollutants in the Aquatic Environment: The Benefits of Upgrading Wastewater Treatment Plants. *Environ. Sci. Technol.* **2014**, *48* (14), 7683−7689.

(16) Suri, R. P. S.; Singh, T. S.; Abburi, S. Influence of alkalinity and salinity on the sonochemical degradation of estrogen hormones in aqueous solution. *Environ. Sci. Technol.* **2010**, *44* (4), 1373−1379.

(17) Frontistis, Z.; Drosou, C.; Tyrovola, K.; Mantzavinos, D.; Fatta-Kassinos, D.; Venieri, D.; Xekoukoulotakis, N. P. Experimental and modeling studies of the degradation of estrogen hormones in aqueous TiO2 suspensions under simulated solar radiation. *Ind. Eng. Chem. Res.* **2012**, *51* (51), 16552−16563.

(18) Filby, A. L.; Shears, J. A.; Drage, B. E.; Churchley, J. H.; Tyler, C. R. Effects of advanced treatments of wastewater effluents on estrogenic and reproductive health impacts in fish. *Environ. Sci. Technol.* **2010**, *44* (11), 4348−4354.

(19) Polubesova, T.; Eldad, S.; Chefetz, B. Adsorption and oxidative transformation of phenolic acids by Fe (III)-montmorillonite. *Environ. Sci. Technol.* **2010**, *44* (11), 4203−4209.

(20) Gu, C.; Li, H.; Teppen, B. J.; Boyd, S. A. Octachlorodibenzo-dioxin formation on Fe (III)-montmorillonite clay. *Environ. Sci. Technol.* **2008**, *42* (13), 4758−4763.

(21) Liyanapatirana, C.; Gwaltney, S. R.; Xia, K. Transformation of triclosan by Fe (III)-saturated montmorillonite. *Environ. Sci. Technol.* **2009**, *44* (2), 668−674.

(22) Lu, J.; Huang, Q.; Mao, L. Removal of acetaminophen using enzyme-mediated oxidative coupling processes: I. Reaction rates and pathways. *Environ. Sci. Technol.* **2009**, *43* (18), 7062−7067.

(23) Allen, B. L.; Hajek, B. F. Mineral Occurrence in Soil Environments. In *Minerals in Soil Environments*, 2nd ed.; Dixon, J. B., Weed, S. B., Eds.; Soil Science Society of America: Madison, 1989; pp 199−278.

(24) Seger, M. R.; Maciel, G. E. NMR investigation of the behavior of an organothiophosphate pesticide, chlorpyrifos, sorbed on montmorillonite clays. *Environ. Sci. Technol.* **2006**, *40* (3), 797−802.

(25) Wei, J.; Furrer, G.; Kaufmann, S.; Schulin, R. Influence of clay minerals on the hydrolysis of carbamate pesticides. *Environ. Sci. Technol.* **2001**, *35* (11), 2226−2232.

(26) Tambach, T. J.; Bolhuis, P. G.; Hensen, E. J. M.; Smit, B. Hysteresis in Clay Swelling Induced by Hydrogen Bonding: Accurate Prediction of Swelling States. *Langmuir* **2005**, *22* (3), 1223−1234.

(27) Grygar, T.; Hradil, D.; Bezdicka, P.; Dousova, B.; Capek, L.; Schneeweiss, O. Fe(III)-modified Montmorillonite and Bentonite: Synthesis, Chemical and UV-Vis spectral Characterization, Arsenic Sorption, and Catalysis of Oxidative Dehydrogenation of Propane. *Clays Clay Miner.* **2007**, *55*, 165−176.

(28) Wallis, P. J.; Chaffee, A. L.; Gates, W. P.; Patti, A. F.; Scott, J. L. Partial Exchange of Fe(III) Montmorillonite with Hexadecyltrimethylammonium Cation Increases Catalytic Activity for Hydrophobic Substrates. *Langmuir* **2009**, *26* (6), 4258−4265.

(29) Boyd, S. A.; Mortland, M. M. Radical formation and polymerization of chlorophenols and chloroanisole on copper(II)-smectite. *Environ. Sci. Technol.* **1986**, *20* (10), 1056−1058.

(30) Gu, C.; Li, H.; Teppen, B. J.; Boyd, S. A. Octachlorodibenzo-dioxin Formation on Fe(III)-Montmorillonite Clay. *Environ. Sci. Technol.* **2008**, *42* (13), 4758−4763.

(31) Arroyo, L. J.; Li, H.; Teppen, B. J.; Boyd, S. A. A simple method for partial purification of reference clays. *Clays Clay Miner.* **2005**, *53* (5), 511−519.

(32) Govindaraj, N.; Mortland, M. M.; Boyd, S. A. Single electron transfer mechanism of oxidative dechlorination of 4-chloroanisole on copper (II)-smectite. *Environ. Sci. Technol.* **1987**, *21* (11), 1119−1123.

(33) Boyd, S. A.; Mortland, M. M. Dioxin radical formation and polymerization on Cu (II)-smectite. *Nature* **1985**, *316* (6028), 532−535.

(34) Boyd, S. A.; Mortland, M. M. Radical formation and polymerization of chlorophenols and chloroanisole on copper (II)-smectite. *Environ. Sci. Technol.* **1986**, *20* (10), 1056−1058.

(35) Mortland, M. M.; Boyd, S. A. Polymerization and dechlorination of chloroethenes on copper (II)-smectite via radical-cation intermediates. *Environ. Sci. Technol.* **1989**, *23* (2), 223−227.

(36) Pal, S.; Bollag, J.-M.; Huang, P. M. Role of abiotic and biotic catalysts in the transformation of phenolic compounds through oxidative coupling reactions. *Soil Biol. Biochem.* **1994**, *26* (7), 813−820.

(37) Gu, C.; Liu, C.; Ding, Y.; Li, H.; Teppen, B. J.; Johnston, C. T.; Boyd, S. A. Clay Mediated Route to Natural Formation of Polychlorodibenzo-p-dioxins. *Environ. Sci. Technol.* **2011**, *45* (8), 3445−3451.

(38) Vantelon, D.; Montarges-Pelletier, E.; Michot, L. J.; Pelletier, M.; Thomas, F.; Briois, V. Iron distribution in the octahedral sheet of dioctahedral smectites. An Fe K-edge X-ray absorption spectroscopy study. *Phys. Chem. Miner.* **2003**, *30* (1), 44−53.

(39) Gu, C.; Liu, C.; Johnston, C. T.; Teppen, B. J.; Li, H.; Boyd, S. A. Pentachlorophenol radical cations generated on Fe(III)-montmorillonite initiate octachlorodibenzo-p-dioxin formation in clays: Density functional theory and fourier transform infrared studies. *Environ. Sci. Technol.* **2011**, *45* (4), 1399−1406.

(40) Zheng, W.; Li, X.; Yates, S. R.; Bradford, S. A. Anaerobic Transformation Kinetics and Mechanism of Steroid Estrogenic Hormones in Dairy Lagoon Water. *Environ. Sci. Technol.* **2012**, *46* (10), 5471−5478.

(41) Mashtare, M. L.; Lee, L. S.; Nies, L. F.; Turco, R. F. Transformation of 17α-estradiol, 17β-estradiol, and estrone in sediments under nitrate-and sulfate-reducing conditions. *Environ. Sci. Technol.* **2013**, *47* (13), 7178−7185.

(42) Mao, L.; Lu, J.; Habteselassie, M.; Luo, Q.; Gao, S.; Cabrera, M.; Huang, Q. Ligninase-mediated removal of natural and synthetic estrogens from water: II. Reactions of 17β-estradiol. *Environ. Sci. Technol.* **2010**, *44* (7), 2599−2604.

(43) Lloret, L.; Eibes, G.; Moreira, M. T.; Feijoo, G.; Lema, J. M. Removal of Estrogenic Compounds from Filtered Secondary Wastewater Effluent in a Continuous Enzymatic Membrane Reactor. Identification of Biotransformation Products. *Environ. Sci. Technol.* **2013**, *47* (9), 4536−4543.

(44) Mao, L.; Huang, Q.; Luo, Q.; Lu, J.; Yang, X.; Gao, S. Ligninase-mediated removal of 17β-estradiol from water in the presence of natural organic matter: Efficiency and pathways. *Chemosphere* **2010**, *80* (4), 469−473.

(45) Pezzella, A.; Lista, L.; Napolitano, A.; d'Ischia, M. Oxidative coupling of 17β-estradiol: inventory of oligomer products and configuration assignment of atropoisomeric C4-linked biphenyl-type dimers and trimers. *J. Org. Chem.* **2004**, *69* (17), 5652−5659.

(46) Nicotra, S.; Intra, A.; Ottolina, G.; Riva, S.; Danieli, B. Laccase-mediated oxidation of the steroid hormone 17β-estradiol in organic solvents. *Tetrahedron: Asymmetry* **2004**, *15* (18), 2927−2931.

(47) Liyanapatirana, C. *Oxidative transformation of antimicrobial compounds by ferric-modified montmorillonite.* http://library.msstate.edu/etd/show.asp?etd=etd-04252011-101445 (accessed Dec 10, 2014).

(48) Hammer, M. J.; Hammer, M. J., Jr. *Water and wastewater Biodegradability of some antibiotics, elimination of the genotoxtechnology,* 4th ed.; Prentice Hall: Upper Saddle River, NJ, 2001.